

## Retrieval of Atmospheric Temperature Profiles from Satellite Measurements for Dynamical Forecasting

W. L. SMITH, H. M. WOOLF AND H. E. FLEMING

*National Environmental Satellite Service, NOAA, Hillcrest Heights, Md.*

(Manuscript received 26 May 1971)

### ABSTRACT

The method of real-time retrieval of atmospheric temperature profiles from Nimbus IV Satellite Infrared Spectrometer observations currently used in dynamical weather analysis-forecast operation is described. Each vertical temperature profile is determined by its deviation from a "guess" profile. The deviation is expressed as a linear combination of differences between the measured radiances and those computed from the guess profile. The coefficients are estimated, by matrix inversion, from the weighting functions (i.e., derivatives of atmospheric transmittance functions), which are regularized by the ratio of the expected variance of the measurement errors to the expected variance of the errors in the guess profile. The deviations are iterated until the variance of the radiance residuals is less than the expected variance of the measurement errors.

For weather analysis-forecast operation the dynamical forecast is used as the first guess; therefore, the calculated profiles should differ from the forecast profiles only when the measurable error in the forecast exceeds the instrumental noise level. The retrieved profiles are those which deviate least from the forecast in order to satisfy all the radiance observations. This property is well suited to dynamical forecasting in that it does not tend to produce erroneous atmospheric waves.

### 1. Introduction

This paper presents the algorithm used to convert Nimbus IV Satellite Infrared Spectrometer (SIRS) observed spectral radiance values into vertical temperature profiles. The algorithm estimates the atmospheric temperature from the measured radiances and a "guess" profile. The solution obtained is that solution which deviates least from the "guess" in order to satisfy all the radiance observations. The algorithm has been applied to SIRS-B radiance values for input into the National Meteorological Center's (NMC) analysis-forecast operation. In this application, the 12-hr forecast is used to construct the "first guess". As a consequence, the resulting solutions represent a correction to the dynamical forecast. Due to the nature of this solution, significant corrections should be obtained only when there is a measurable error in the guess; that is, when the observed radiances differ from those which would arise from the forecast atmosphere by more than the instrumental noise level. This solution should be optimal for dynamical forecasting in the sense that it does not tend to produce erroneous atmospheric waves. Results are shown which illustrate the effectiveness of this method in correcting a dynamical forecast on the basis of satellite measured radiances.

For other applications, relatively accurate temperature profiles can be obtained using a more arbitrary first "guess", such as a climatological profile. Results

are given which indicate that for clear sky conditions the temperature profile can be specified accurately by this method (i.e., temperature errors  $< \pm 3\text{C}$ ), regardless of the representativeness of the climatological guess. The absolute specification of accuracy increases rapidly with increasing precision of the guess profile.

### 2. Measurement characteristics

The second version of the Satellite Infrared Spectrometer, SIRS-B, was developed by D. Q. Wark and D. T. Hilleary of the National Environmental Satellite Service (Wark and Hilleary, 1969). Briefly, the SIRS-B aboard the Nimbus IV satellite measures the radiance leaving the earth-atmosphere system in seven spectral intervals of the 15- $\mu\text{m}$   $\text{CO}_2$  band, one spectral interval of the 11- $\mu\text{m}$  window region, and six spectral intervals of the rotational water vapor absorption band. Each spectral interval is 5  $\text{cm}^{-1}$  wide. Table 1 gives the central positions of the SIRS-B channels. Further details can be found in the *Nimbus IV User's Guide* (1970).

The outgoing radiance from earth measured by any channel of SIRS is related to the atmosphere's tempera-

TABLE 1. Central spectral positions of SIRS-B channels ( $\text{cm}^{-1}$ ).

11- $\mu\text{m}$ "window"	899.0						
15- $\mu\text{m}$ $\text{CO}_2$	750.0	734.0	709.0	701.0	692.0	679.8	668.7
Rotational $\text{H}_2\text{O}$	531.5	436.5	425.5	291.5	302.0	280.0	

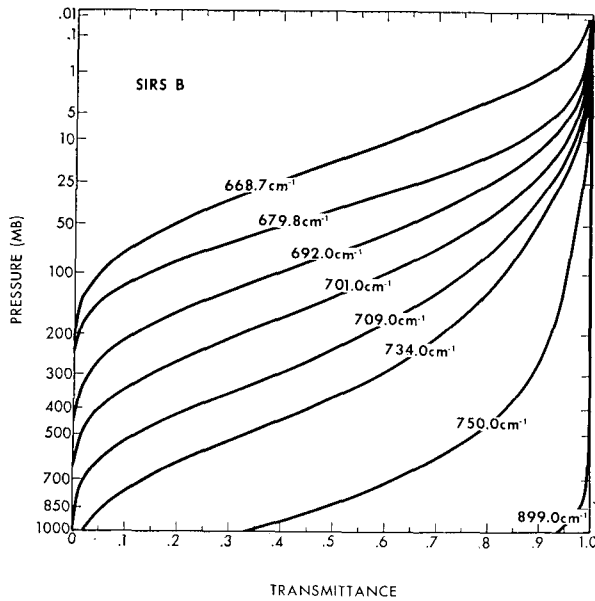


FIG. 1. SIRS-B atmospheric transmission functions for a mid-latitude atmosphere.

ture and absorbing gas structure by the radiative transfer equation

$$N(\nu) = B_\nu[T(p_0)]\tau_\nu(p_0) - \int_0^{p_0} B_\nu[T(p)] \frac{d\tau_\nu(p)}{dx(p)} dx(p), \quad (1)$$

where  $N(\nu)$  is the outgoing spectral radiance within a spectral channel centered at frequency  $\nu$ ,  $B_\nu$  the Planck radiance for temperature  $T(p)$  at pressure  $p$ ,  $\tau_\nu(p)$  the transmittance of the atmosphere above pressure  $p$ , and  $x(p)$  is an arbitrary function of pressure. [Throughout, 100 levels scaled by  $p^{2/7}$  are adopted for  $x(p)$  to minimize

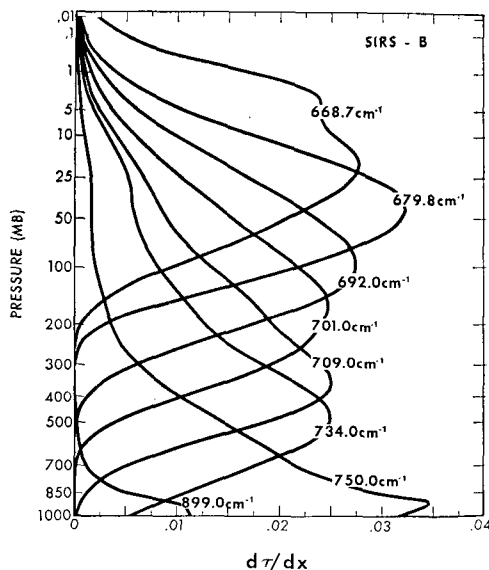


FIG. 2. Derivative of transmittance with respect to  $x(p) \propto p^{2/7}$ .

errors of quadrature.] The 15- $\mu\text{m}$   $\text{CO}_2$  channels are used for atmospheric temperature profiling. Since the distribution of  $\text{CO}_2$  is known [i.e., a uniform optical depth of 0.247 atm-cm ( $\text{mb}^{-1}$ )], the  $\text{CO}_2$  channel transmittances can be estimated (Wark, 1970). The spectral radiances measured in the  $\text{CO}_2$  band can be interpreted in terms of the temperature profile from the solution of Eq. (1).

Figs. 1 and 2 show the SIRS-B  $\text{CO}_2$  channel atmospheric transmittances computed for a mid-latitude atmosphere, and their derivatives with respect to  $x(p) \propto p^{2/7}$ . The derivatives are in the weighting functions of the radiative transfer equation (1). As such they display the relative sensitivity of measured radiance in each channel to the temperature variations in various vertical layers of the atmosphere. The 669  $\text{cm}^{-1}$  channel, which senses the radiation transferred through the atmosphere in the strongest absorbing portion of the 15- $\mu\text{m}$   $\text{CO}_2$  band, is most highly sensitive to the temperature variations in the middle stratosphere. The spectral channels which sense the radiation transferred through the atmosphere in weaker absorbing regions of the 15- $\mu\text{m}$   $\text{CO}_2$  band, are most highly sensitive to the temperature variations in lower atmospheric layers. Most of the radiance measured in the 11- $\mu\text{m}$  window arises from the earth's surface. It is the vertical independence of the earth's outgoing radiation in the different spectral channels which allows one to determine a solution of the vertical temperature profile throughout its entire extent.

### 3. The analytical solution

The solution of the radiative transfer equation for the temperature profile developed here is similar to the solution of this type of integral equation presented by Foster (1961) and Twomey (1963). The problem is to solve (1) for  $T(p)$  given the finite set of measurements  $N(\nu)$ , obtained for the SIRS-B 15- $\mu\text{m}$   $\text{CO}_2$  spectral intervals.

The solution of (1) for  $T(p)$  first requires separating variables in the Planck function. This can be accomplished by normalizing the measured spectral radiances at the frequency  $\nu$  to their blackbody equivalent at some reference frequency through Planck's equation, i.e.,

$$N_r(\nu) = B_r[T_B(\nu)] = C_1 \nu^3 / \{\exp[C_2 \nu / T_B(\nu)] - 1\},$$

where

$$C_1 = 1.19061 \times 10^{-5} \text{ erg (cm}^2\text{-sec-sr cm}^{-1}\text{)}^{-1},$$

$$C_2 = 1.43868 \text{ cm (}^\circ\text{K)},$$

and  $T_B(\nu)$ , the brightness temperature corresponding to the measured radiance  $N(\nu)$ , is given by

$$T_B(\nu) = C_2 \nu / \ln\{[C_1 \nu^3 / N(\nu)] + 1\}.$$

Eq. (1) may now be rewritten for the reference fre

quency  $r$  as

$$N_r(\nu) = B_r[T(\rho_0)]_{\tau_r(\rho_0)} - \int_0^{\rho_0} B_r[T(\rho)] \frac{d\tau_r(\rho)}{dx(\rho)} dx(\rho), \quad (2)$$

and is linear in  $B_r[T(\rho)]$ . The solution of (2) for  $T(\rho)$  simply requires a solution for  $B_r[T(\rho)]$  and then the direct calculation of  $T(\rho)$  from  $B_r[T(\rho)]$ , using the inverse of Planck's equation, i.e.,

$$T = C_2 r / \ln[(C_1 r^3 / B_r) + 1].$$

Using the guess profile, one can approximate (2) by numerical quadrature and write it as a perturbed equation of the form

$$N_i' = \sum_{j=1}^J \Gamma_{ij} B_j', \quad i = 1, 2, \dots, M, \quad (3)$$

where  $M$  is the number of different spectral radiance observations ( $M \leq 8$  for SIRS applications) and  $J$  the number of discrete pressure levels equally spaced in  $x(\rho) \propto \rho^{2/7}$ . The prime denotes the deviation of the true value from a "guess" value. The trapezoidal rule is used so that

$$\Gamma_{ij} = 0.5 \times \begin{cases} [\tau_{i,j} - \tau_{i,j+1}], & j = 1 \\ [\tau_{i,j-1} - \tau_{i,j+1}], & 1 < j < J \\ [\tau_{i,j-1} + \tau_{i,j}], & j = J = 100 \end{cases}$$

The top of the atmosphere corresponds to  $j=1$  and the surface to  $j=J$ . The guessed temperature profile is applied to (2) to obtain the "guessed" radiance. Writing (3) in matrix notation, one obtains

$$\mathbf{n} = \mathbf{\Gamma} \mathbf{b}, \quad (4)$$

where  $\mathbf{n}$  is a column vector of the radiance deviations (the error in the guessed radiance),  $\mathbf{b}$  a column vector of Planck radiance departures from their respective guessed values (i.e., the error of the guessed Planck radiance profile), and  $\mathbf{\Gamma}[\tau_{ij}]$  the matrix of transmittance functions.

Because  $\mathbf{\Gamma}$  is a rectangular matrix of dimension  $M \times J$  with  $J > M$ , (4) has an infinite number of solutions. Solving this problem in a least-squares sense, that is, minimizing the quadratic form  $(\mathbf{\Gamma} \mathbf{b} - \mathbf{n})^T (\mathbf{\Gamma} \mathbf{b} - \mathbf{n})$  does not alleviate the non-uniqueness problem. (The superscript  $T$  denotes the transpose.) As stated earlier, we wish to obtain that solution of (4) which deviates least in the squared sense from the guessed profile. In other words, we want that solution  $\mathbf{b}$  which minimizes the quadratic form

$$F(\mathbf{b}) = (\mathbf{\Gamma} \mathbf{b} - \mathbf{n})^T (\mathbf{\Gamma} \mathbf{b} - \mathbf{n}) + \gamma \mathbf{b}^T \mathbf{b}, \quad (5)$$

where  $\gamma$  is a Lagrangian multiplier. Differentiation with respect to the elements of  $\mathbf{b}$  yields the normal equation

$$(\mathbf{\Gamma}^T \mathbf{\Gamma} + \gamma \mathbf{I}) \mathbf{b} = \mathbf{\Gamma}^T \mathbf{n}, \quad (6)$$

which has the unique solution

$$\hat{\mathbf{b}} = (\mathbf{\Gamma}^T \mathbf{\Gamma} + \gamma \mathbf{I})^{-1} \mathbf{\Gamma}^T \mathbf{n}, \quad (7)$$

for  $\gamma > 0$ , where  $\mathbf{I}$  is the identity matrix. Because  $\mathbf{\Gamma}$  has dimensions  $M \times J$  with  $J > M$ , the inverse matrix in (7) is of dimension  $J \times J$ . There is no need to invert such a large matrix. The identity

$$(\mathbf{\Gamma}^T \mathbf{\Gamma} + \gamma \mathbf{I})^{-1} \mathbf{\Gamma}^T = \mathbf{\Gamma}^T (\mathbf{\Gamma} \mathbf{\Gamma}^T + \gamma \mathbf{I})^{-1}$$

may be applied to (7) to obtain

$$\hat{\mathbf{b}} = \mathbf{\Gamma}^T (\mathbf{\Gamma} \mathbf{\Gamma}^T + \gamma \mathbf{I})^{-1} \mathbf{n} = \mathbf{C} \mathbf{n}, \quad (8)$$

which requires the inverse of the smaller  $M \times M$  matrix.

To this point nothing has been said about the value of the scalar  $\gamma$  which arose in this problem as a Lagrangian multiplier. In order to assign a value to  $\gamma$ , we must find what  $\gamma$  means physically. To decide this, we refer to the paper by Smith *et al.* (1970). Following the derivation presented there, which is based on statistical concepts, we find that

$$\hat{\mathbf{b}} = (\mathbf{B} \mathbf{B}^T) \mathbf{\Gamma}^T [\mathbf{\Gamma} (\mathbf{B} \mathbf{B}^T) \mathbf{\Gamma}^T + \mathbf{E} \mathbf{E}^T]^{-1} \mathbf{n}, \quad (9)$$

where  $\mathbf{B} \mathbf{B}^T$  is the covariance matrix of a statistical set of deviations of Planck radiance (temperature) profiles from realistic guess profiles and  $\mathbf{E} \mathbf{E}^T$  the covariance matrix of the observational errors.

Comparison of (8) and (9) indicates that (9) is a more general solution than (8). However, (9) is impractical since actual covariances of the errors of particular guess profiles (the elements of  $\mathbf{B} \mathbf{B}^T$ ) are difficult to estimate. This is so because the guess profiles to be used routinely are obtained from a dynamical forecast. The statistics obtained from a sample of conventional temperature profile observations and forecast profiles would not be representative of regions where conventional data are sparse. However, simplifying assumptions about these covariances can be made which tend to be satisfied as the guess profile approaches the true profile. The assumptions are 1) that the errors of the guess are random, and 2) that the expected value of the variance of the guess error is the same for all pressure levels. Under these assumptions and the assumption of random radiance measurement error, the minimum information conditions

$$\mathbf{B} \mathbf{B}^T = \sigma_b^2 \mathbf{I}, \quad (10)$$

$$\mathbf{E} \mathbf{E}^T = \sigma_e^2 \mathbf{I}, \quad (11)$$

result. The scalars  $\sigma_b^2$  and  $\sigma_e^2$  are the error variances and are called "signal power" and "noise power" respectively by Foster (1961). It follows from substituting (10) and (11) into (9) that

$$\hat{\mathbf{b}} = \mathbf{\Gamma}^T [\mathbf{\Gamma} \mathbf{\Gamma}^T + (\sigma_e^2 / \sigma_b^2) \mathbf{I}]^{-1} \mathbf{n} = \mathbf{C} \mathbf{n}, \quad (12)$$

which is identical to (8) with

$$\gamma = \frac{\sigma_e^2}{\sigma_b^2}. \quad (13)$$

Thus,  $\gamma$  is the ratio of noise to signal power. For any individual situation  $\gamma$  is not known. Consequently, a sta-

tistically expected value must be utilized. Assuming the standard error  $\sigma_e$  of the SIRS measurements to be  $0.25 \text{ erg (cm}^2\text{-sec-sr cm}^{-1})^{-1}$ , as determined from calibration data, and a standard error  $\sigma_b$  of an arbitrary guess to be  $8 \text{ ergs (cm}^2\text{-sec-sr cm}^{-1})^{-1}$ , which corresponds to the average standard deviation of atmospheric temperature, then  $\gamma \approx 10^{-3}$ .

Use of an unrepresentative  $\gamma$  value in (8) can restrict the solution for the temperature profile such that the solution profile will not necessarily satisfy the observed radiances to within their error level. However, such a restriction can be overcome by simply iterating (8), at each step using the previous solution as the "guess" profile, until the radiance residuals (differences between those observed and those computed from the guess profile) are reduced to the noise level. Convergence is defined as that condition in which

$$\frac{1}{M} \sum_{i=1}^M [N_r^j(\nu_i) - N_r(\nu_i)]^2 \leq \sigma_e^2, \quad (14)$$

where  $N_r^j(\nu_i)$  is the radiance computed from the  $j$ th profile solution for the  $i$ th spectral channel. Since  $\mathbf{b} \rightarrow 0$  as  $\mathbf{n} \rightarrow 0$ , regardless of  $C$ , it is obvious the errors in  $\mathbf{b}$  resulting from errors in  $\gamma$  decrease as the radiance residuals decrease to the noise level. As a consequence, the

solution will converge as long as the solution obtained at the first iterative step is more accurate than the initial guess. It has been found by experience that an order-of-magnitude estimate of  $\gamma$  is sufficient for achieving rapid convergence.

#### 4. Solution characteristics

The solution given by (8) can be written in the computational form

$$B_r[T(p_j)] = B_r[\hat{T}(p_j)] + \sum_{i=1}^8 C(\nu_i, p_j) N_r'(\nu_i), \quad j=1, 2, \dots, 100, \quad (15)$$

where  $N_r'(\nu_i) = N_r(\nu_i) - \hat{N}_r(\nu_i)$ ,  $B_r[\hat{T}(p_j)]$  is the Planck radiance corresponding to the guess temperature at the  $p_j$  pressure level,  $\hat{N}_r(\nu_i)$  the radiance calculated from the guess temperature profile, and the  $C(\nu_i, p_j)$  coefficients are the elements of the  $\mathbf{C}$  matrix given in (12). It is seen from (12) that the coefficients are a function of the atmospheric transmittances and the ratio of the measurement error variance to the temperature error (Planck radiance error) variance.

Fig. 3 shows the  $C(\nu_i, p_j)$  coefficients computed from a set of mid-latitude atmospheric transmittances and

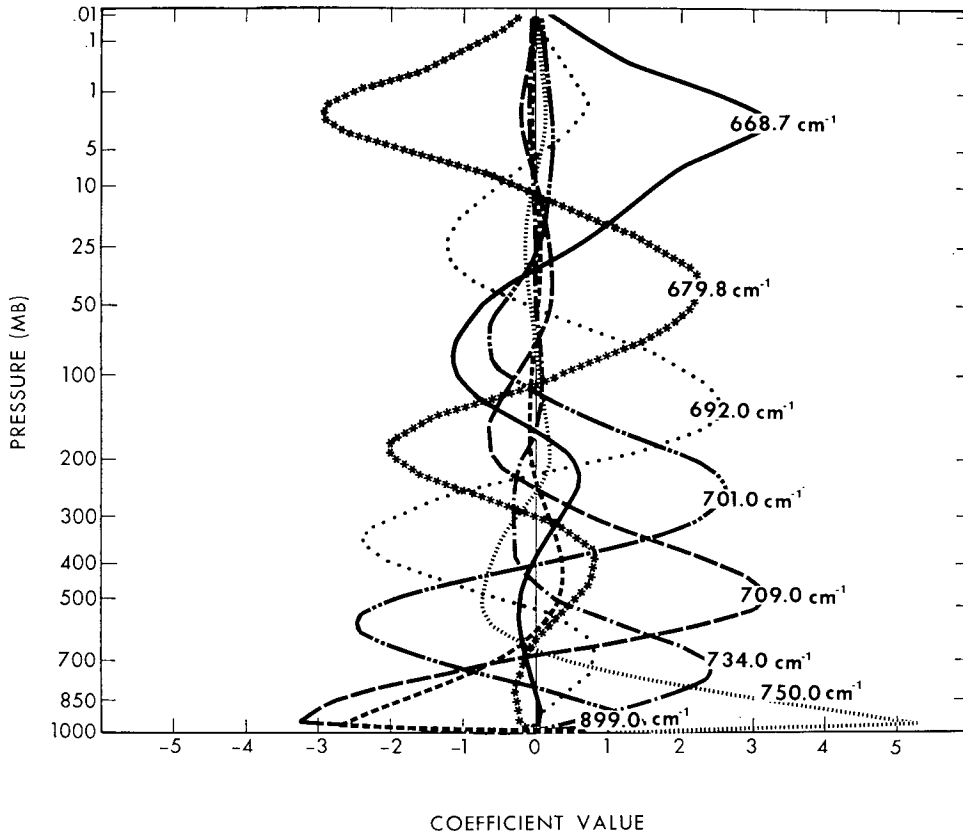


FIG. 3. Solution coefficients computed from a set of mid-latitude atmospheric transmittances.

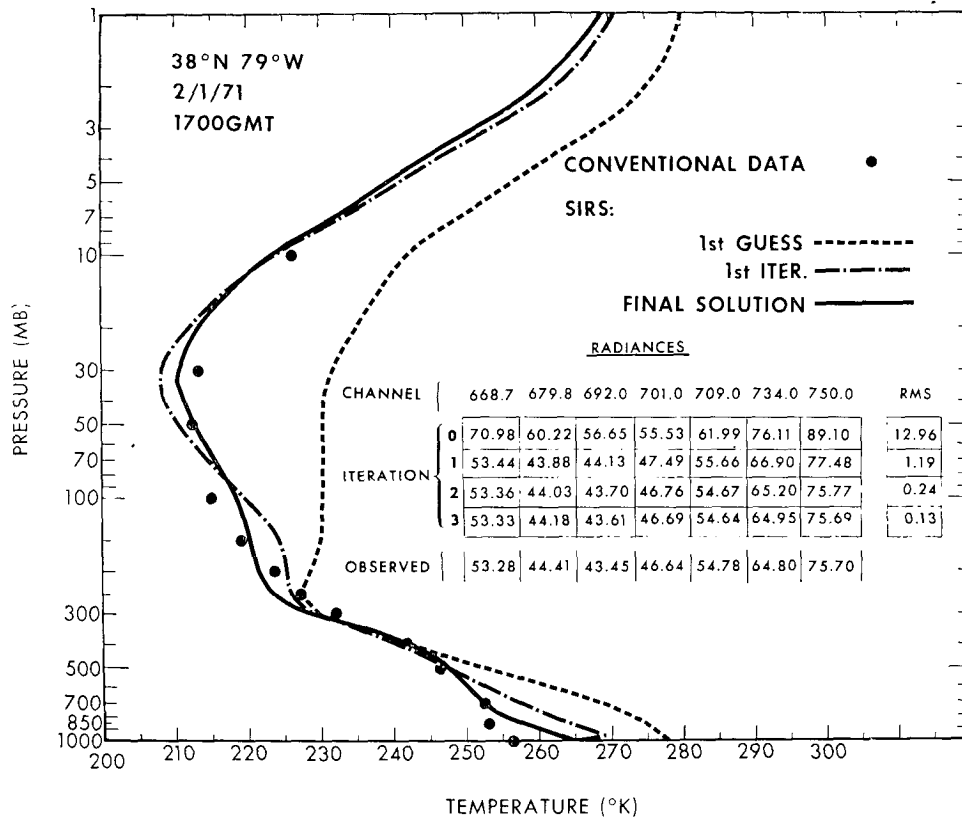


Fig. 4. Comparison of a SIRS-B derived temperature profile and conventional data. Table inset shows calculated radiances and radiance residuals as a function of iterative step.

a  $\gamma$  value of  $10^{-3}$ . These coefficient functions are the radiance weighting functions in the temperature profile solution (15). As may be seen each spectral radiance has a pressure level of maximum influence. These radiance weighting functions dampen out slowly with pressure as one moves away from the levels of maximum influence; therefore, each spectral radiance value will impact the temperature solution to some degree at every level of the atmosphere. The overlapping positive and negative modes of the weighting functions display the lack of vertical independence of the various spectral radiance measurements.

Fig. 4 shows a temperature profile solution from SIRS-B mid-latitude radiances whose initial guess is a climatological temperature profile. As can be seen, the convergence is rapid; it was achieved in three steps from a relatively poor initial guess. The table inset in Fig. 4, which shows the calculated radiances and radiance residuals as a function of iterative step, illustrates the very high convergence rate of this solution. The discrepancies between the SIRS solution and radiosonde (conventional) data in the lower troposphere is due to the 5-hr time difference of the two observations. (The SIRS observation is at 1700 GMT whereas the radiosonde observation is at 1200.)

As shown earlier, the solution given by (12) is that

which perturbs the initial guess least in order to satisfy all the radiance observations. But, if a different initial guess is used with the same radiances, then a different solution can be expected. The dependence on the initial guess can be investigated by comparing solutions obtained from a single set of radiance observations and a variety of initial guess profiles. Figs. 6 and 7 show such comparisons obtained from SIRS-B radiance observations using the *U. S. Standard Atmosphere Supplements* shown in Fig. 5 as guessed profiles. Comparison of the solutions with conventional radiosonde data shows that the reproduction of the gross characteristics of the atmosphere's vertical temperature structure is quite good regardless of the initial profile employed. The envelope of differences of the various solutions has a half-width of about 3C except near the earth's surface where larger errors apparently result from very poor guessed profiles, and above 30 mb where the information content of the radiances is relatively small. The most accurate solutions, of course, are those resulting from the standard atmosphere profiles whose vertical characteristics most closely resembled those of the true profile.

Clouds generally exist within the relatively large field of view (i.e., 225 km square) of SIRS. Since clouds tend to be opaque to infrared radiation, severe errors in the calculated temperature profile below the cloud level will

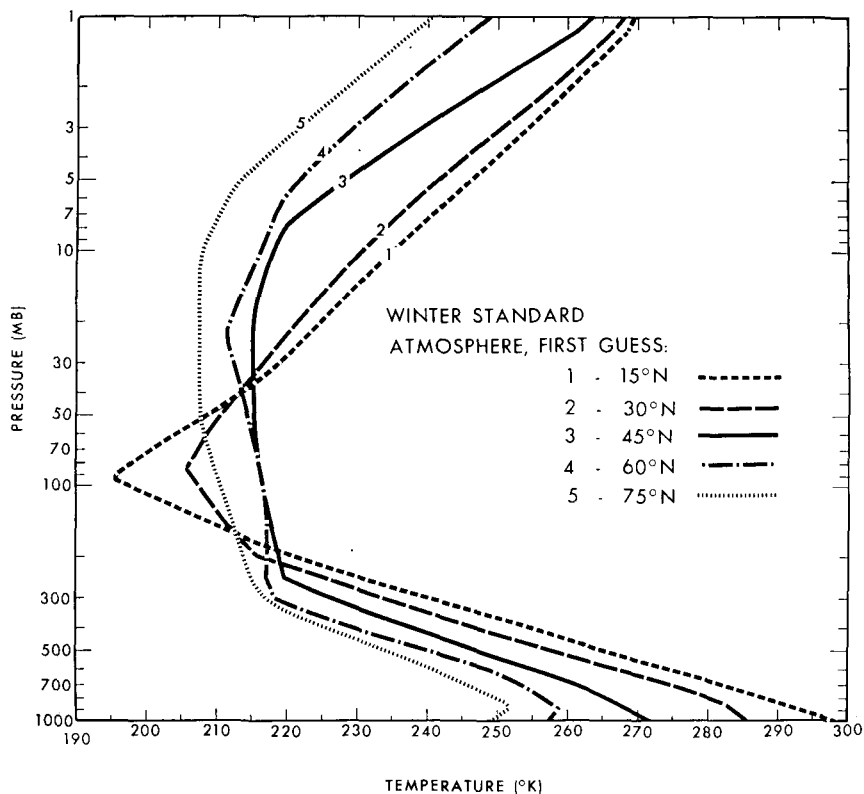


FIG. 5. Winter temperature profiles from *U.S. Standard Atmosphere Supplements* for 15, 30, 45, 60 and 75N.

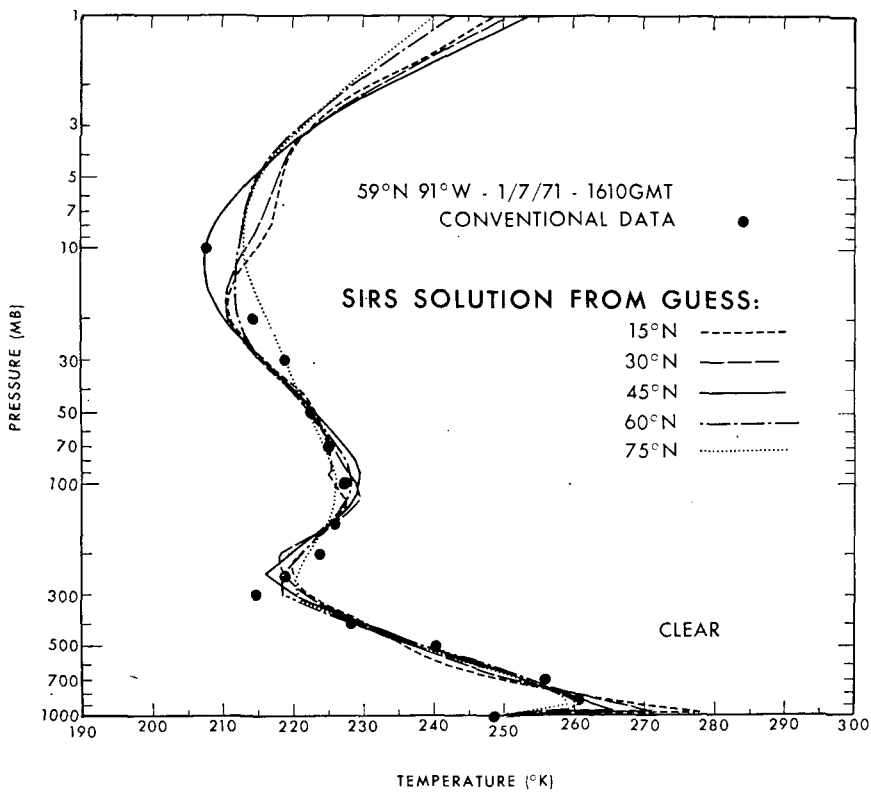


FIG. 6. High-latitude comparison between the SIRS-B derived temperature profiles (using the *U.S. Standard Atmosphere Supplements* guesses shown in Fig. 5), and conventional data.

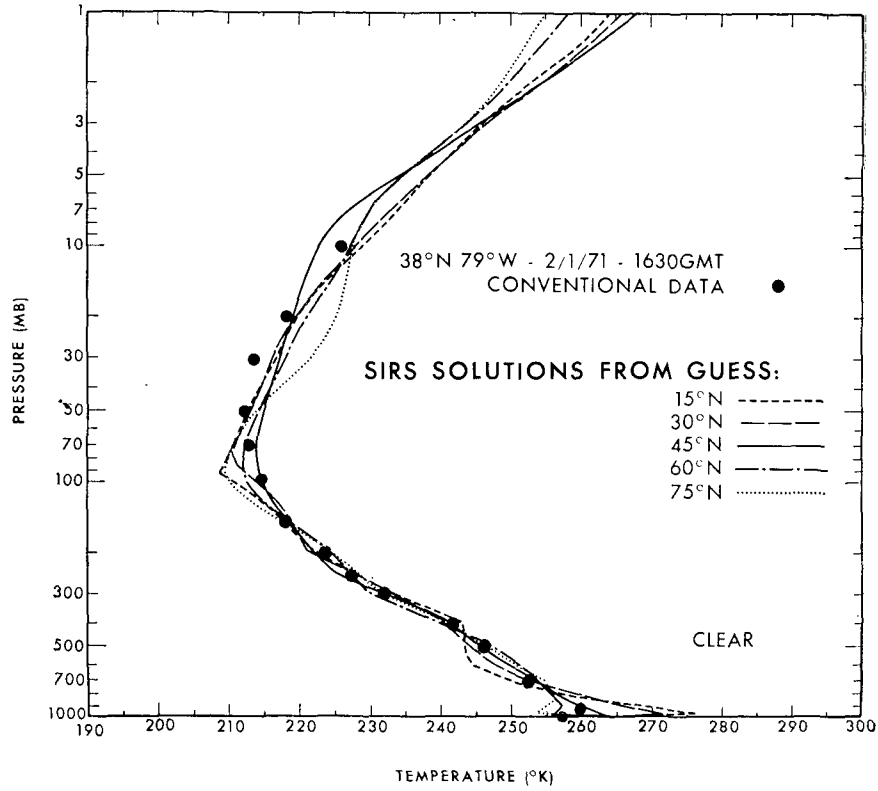


Fig. 7. Mid-latitude comparison between the SIRS-B derived temperature profiles (using the *U.S. Standard Atmosphere Supplements* guesses shown in Fig. 5) and conventional data.

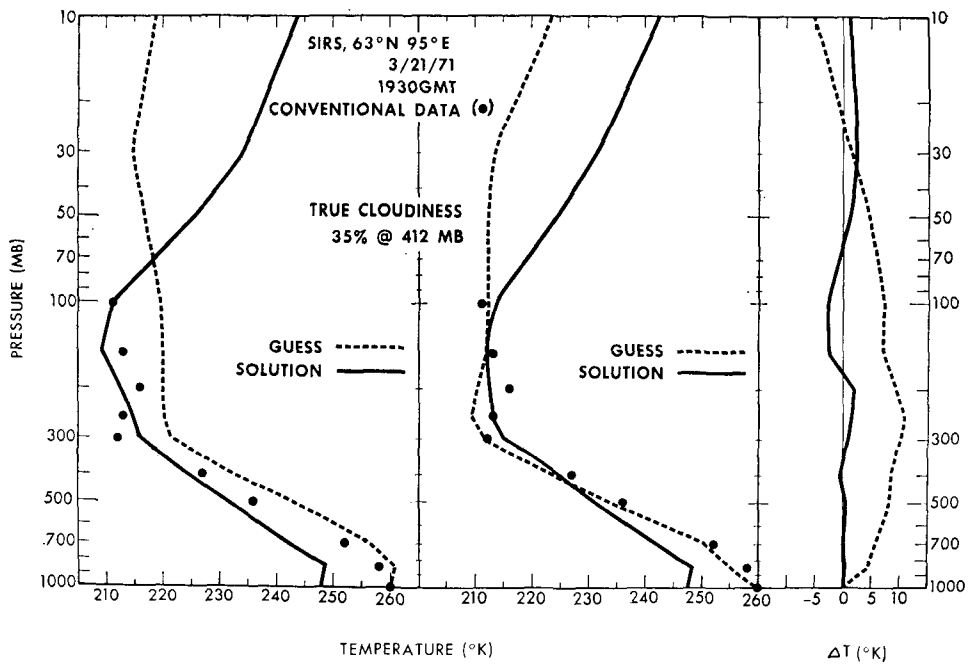


Fig. 8. SIRS-B temperature profiles derived from a set of cloud contaminated radiances. Clear sky conditions were assumed and two different climatological guess profiles were used. The  $\Delta T$  curves are the difference between the two solutions (solid line) and the difference between the two guesses (dashed line).

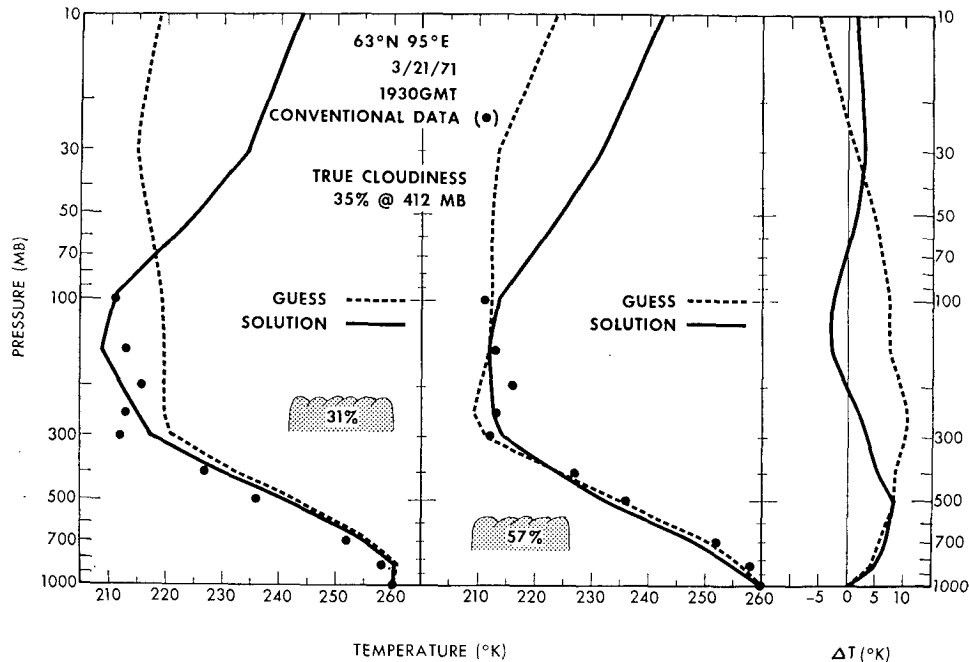


FIG. 9. SIRS-B temperature profiles obtained by applying the cloud correction technique. The  $\Delta T$  curves are the difference between the two solutions (solid line) and the difference between the two guesses (dashed line).

result if their radiative effects are neglected in the solutions.

Fig. 8 shows temperature profile solutions obtained from one set of cloud-contaminated SIRS-B radiances and two different guessed profiles under the assumption that the atmosphere was clear. Both solutions are reasonably good down to the cloud level of 412 mb (as determined from the radiances and the radiosonde observation). Below the cloud level the calculated temperatures are too low due to the attenuation of the radiances by the cloud. The difference curves (between guesses and between solutions) on the right-hand side of Fig. 8 show that the two solutions are nearly identical, even though the two guesses were significantly different. (The two guessed profiles used were the climatological profiles indicated in Fig. 5 translated so that their surface temperature equalled the surface radiosonde value.)

Smith *et al.* (1970) give a procedure for correcting SIRS measured radiances for the effects of clouds. The cloud corrections depend upon the height and the amount of clouds. The two most transparent  $\text{CO}_2$  channels (i.e., 734 and 750  $\text{cm}^{-1}$ ) and the window (899  $\text{cm}^{-1}$ ) channel must be used to calculate the heights and amounts of cloud within the field of view on the basis of the guess temperature profile. The cloud-corrected radiances are used to calculate the temperature profile. The cloud corrections can be improved by iteration if the profile computed at each step is used to calculate new cloud parameters.

Fig. 9 shows the effect of applying the cloud-correction technique to the temperature profile solution for

the cases illustrated in Fig. 8. The calculated amount of cloudiness is shown in each case. The solution below the true cloud level is very dependent on the guess profile. This is most clearly illustrated by comparing the two solution differences with the two initial guess differences. The differences are nearly identical below the true cloud level. The lack of uniqueness in the cloudy sky solution is due to the nonlinear relation between outgoing radiance and cloud height, cloud amount, and atmospheric temperature. It is evident in Fig. 9 that high clouds with warm tropospheric temperature and low clouds with cold tropospheric temperatures both satisfy the radiance observations for intermediate cloud and temperature conditions.

Significant improvements on the initial guess below clouds could be obtained if the correct cloud conditions were known from independent data. The two solutions obtained for the case discussed above when the cloud cover was 35% at 412 mb (as specified by radiance and radiosonde measurements) agreed to within 1C of the tropospheric radiosonde data.

Since independent cloud data for the SIRS field of view cannot be obtained on an operational basis, the cloud parameters must be calculated from the SIRS radiances. Consequently, the accuracy of the solution below the cloud is very dependent on the accuracy of the initial guess. Fortunately, clear-column radiances will be able to be derived independently of a guess temperature profile from data obtained with future ITOS and Nimbus high-spatial-resolution scanning infrared sounders (Smith, 1969, 1971). With these measure-



ments, profiles with the accuracy obtained under cloudless conditions will be achievable down to the earth's surface under partially cloudy sky conditions.

### 5. Application to the analysis-forecast operation

The algorithm for retrieving temperature profiles presented above has been applied to Nimbus-IV SIRS-B data on a routine basis since 14 June 1970. Data are processed four times a day for use in the 0000 and 1200 GMT NMC isobaric analyses. For each synoptic period the same radiance data are processed twice, once for *operational* analyses which are produced 3 hr after the synoptic time, and again for the *final* analyses which are produced 10 hr after synoptic time.

The retrieval temperature profiles (hereafter called the *operational* and *final* soundings) for the operational and final analyses are not identical because, although the radiances are identical for each sounding, the first guess temperature profiles are different. For the operational sounding, the NMC 12-hr tropospheric forecast is used to construct the first guess in the transformation of radiances to temperatures. For the final sounding, the NMC operational tropospheric analyses (which contain the conventional synoptic data and the operational soundings) are used to construct the first guess profile. For both the operational and final data processing, the latest available daily stratospheric analyses are used to construct the first guess profile above the 100-mb level and up to the 10-mb level. The *U. S. Standard Atmosphere Supplements* are used to provide a representative seasonal and latitudinal first guess above the 10-mb level.

Fig. 10 shows an example of an operational SIRS-B sounding which departed significantly from the 12-hr forecast. The changes indicated by the sounding are corroborated by the NMC analyses of conventional radiosonde data. (There were several radiosondes in this region so that the NMC analysis was influenced primarily by the radiosonde data and not by this single SIRS sounding.)

It is difficult, in general, to verify the improvement of the NMC analyses through the use of SIRS data. In the first place, the errors of the 12-hr forecast tend to be small in regions where radiosonde (verifying) data are numerous. In fact, in dense data areas, the errors of the forecast are generally not much larger than the radiosonde observational errors. Second, the SIRS data are asynoptic, having been obtained near local noon or midnight from the sun-synchronous Nimbus satellite. The combined influence of radiosonde errors and discrepancies due to time differences between SIRS and radiosonde observations makes it difficult to verify that the SIRS temperatures are significantly better than those from 12-hr forecasts.

Table 2 shows SIRS verification statistics for the 200-, 300- and 500-mb levels for January 1971 provided by Hayden and Broderick (personal communication). The

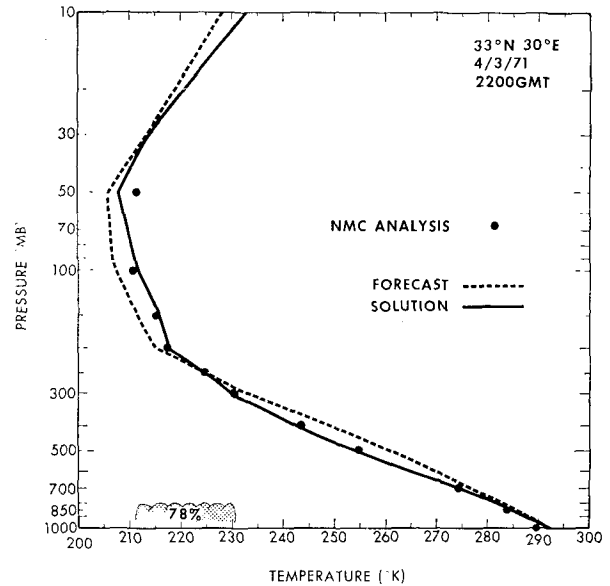


FIG. 10. SIRS-B derived temperature profile, using the NMC 12-hr forecast as the initial guess.

statistics were designed to investigate to what degree the operational soundings are able to correct the 12-hr forecast error. They were compiled from data obtained in regions having a dense network of radiosonde stations. The operational SIRS solutions were verified on the basis of two estimates of the "true" temperature: (i) NMC analyses interpolated in space and time to the SIRS observation; and (ii) the final SIRS solution which utilizes (i) as the initial guess. Both estimates are imperfect: estimate (i) contains errors from radiosonde data and from the time interpolation, whereas estimate (ii) is not an independent standard. However, as shown in Table 2, the forecast errors implied by both estimates of the truth are highly correlated (correlation coefficient  $r_1$  of Table 2) and have an rms discrepancy of about 1C.

Table 2 shows the correlations of the forecast errors implied by the operational soundings (SIRS temperature minus forecast temperature) with the "true" forecast errors implied by estimates (i) and (ii) (estimate minus forecast temperature). The correlations show that the adjustments made by the operational soundings are generally in the proper direction, regardless of which estimate of the truth is used. The improvement of the operational SIRS data over the forecast, as indicated by the differences of the forecast and SIRS standard errors, depends somewhat on the estimate of the true atmospheric state, especially for the 300- and 500-mb levels. However, for both estimates, the standard error of the operational soundings, as indicated by  $\sigma_s$ , is significantly less than the forecast error at the 200-mb level for all cloud conditions and at the 300- and 500-mb levels for clear sky conditions. All the statistics reveal the expected decrease of SIRS information content at the lower levels with increasing SIRS-derived cloud height.

TABLE 2. SIRS verification statistics for January 1971.

	Comparison of standards			Forecast and SIRS errors based on RAOB standard				Forecast and SIRS errors based on final SIRS standard			
	Pressure (mb)	rms	$r_1$	Forecast $\sigma_e$	SIRS $\sigma_e$	Difference	$r_2$	Forecast $\sigma_e$	SIRS $\sigma_e$	Difference	$r_3$
All Cases	200	1.2	0.96	3.6	2.4	1.2	0.75	3.9	2.1	1.8	0.87
Clear	200	0.8	0.98	3.1	1.8	1.3	0.82	3.6	1.8	1.8	0.87
Low Cloud	200	1.2	0.93	2.8	2.2	0.6	0.64	3.1	1.7	1.4	0.84
Middle and High Cloud	200	1.2	0.96	4.0	2.5	1.5	0.79	4.3	2.3	2.0	0.89
All Cases	300	0.9	0.91	1.9	1.9	0.0	0.46	2.2	1.7	0.5	0.66
Clear	300	0.7	0.97	1.9	1.2	0.7	0.78	2.3	1.2	1.1	0.86
Low Cloud	300	1.0	0.91	1.9	1.9	0.0	0.41	2.2	1.6	0.6	0.62
Middle and High Cloud	300	1.0	0.90	1.8	1.9	-0.1	0.41	2.2	1.7	0.5	0.62
All Cases	500	1.3	0.84	1.4	1.6	-0.2	0.71	2.2	1.3	0.9	0.82
Clear	500	1.0	0.91	1.6	1.1	0.5	0.88	2.2	0.9	1.3	0.91
Low Cloud	500	0.8	0.91	1.4	1.1	0.3	0.72	1.8	0.9	0.9	0.88
Middle and High Cloud	500	1.5	0.82	1.4	1.6	-0.2	0.69	2.3	1.5	0.8	0.79

$r_1$  = correlation of the raob indicated forecast error with the final SIRS indicated forecast error.

$r_2$  = correlation of the operational SIRS derived forecast error with the raob indicated forecast error.

$r_3$  = correlation of the operational SIRS derived forecast error with the final SIRS indicated forecast.

$\sigma_e$  = rms error ( $^{\circ}$ C).

The relatively poor accuracy at the 300-mb level is probably due to the lack of sufficient vertical resolution for defining the tropopause level and temperature. (The  $692\text{ cm}^{-1}$  channel radiance observations were excessively noisy during this period and consequently could not be used in the derivation of the temperature profiles. A significant loss in tropopause temperature resolution resulted from the loss of this channel.)

## 6. Summary and conclusions

An algorithm has been presented for retrieving temperature profiles from satellite radiance measurements. The particular solution obtained, of the infinite number possible, is that one which deviates least from the initial guess in order to satisfy the observed radiance observations. This type of solution appears optimal when using a dynamical forecast as an initial guess. The solution does not tend to produce erroneous atmospheric waves which could arise from radiance measurement errors or from the non-uniqueness of the inverse solution of the radiative transfer equation.

This algorithm has been used to process SIRS-B radiance data for the NMC analysis-forecast operation. Verification statistics indicate that the SIRS-derived temperatures are in most cases significantly better than those from the 12-hr forecast.

The major limitation of this method, as applied to SIRS measurements, is the non-uniqueness and resulting bias of the tropospheric temperature solution induced by partial cloudiness. This limitation should be overcome with the next generation ITOS and Nimbus sounding radiometers which have the necessary spatial resolution and scan geometry for defining the clear air radiances over a partly cloudy region.

*Acknowledgments.* We wish to thank Dr. D. Q. Wark, Mr. D. T. Hilleary, Mr. James Lienesch, and Mr. Spencer Anderson for continuously providing the SIRS measurements in the form and with the reliability needed for operational usage. We also appreciate the contributions of Drs. D. Q. Wark, C. Hayden, S. Fritz, J. Winston and D. Crosby, in the application of SIRS measurements to the analysis-forecast operation. We acknowledge the assistance of P. Pellegrino, L. Mannello and R. Ryan in the task of monitoring the SIRS temperature profile data on a daily basis.

## REFERENCES

- Foster, M., 1961: An application of the Wiener-Kolmogorov smoothing theory to matrix inversion. *J. Soc. Ind. Appl. Math.*, **9**, 387-392.
- Nimbus Project, 1970: *The Nimbus IV User's Guide*. Goddard Space Flight Center, NASA, 214 pp.
- Smith, W. L., 1969: The improvement of clear column radiance determination with a supplementary  $3.8\text{ }\mu\text{m}$  window channel. ESSA Tech. Memo. NESCTM 16, 17 pp (available from the National Technical Information Service).
- , 1971: Calculation of clear column radiances using airborne infrared temperature profile radiometer measurements over partly cloudy areas. NOAA Tech. Memo. NESS 28, 12 pp (available from the National Technical Information Service).
- , H. M. Woolf and W. J. Jacob, 1970: A regression method for obtaining real time temperature and geopotential height profiles from satellite spectrometer measurements and its application to Nimbus III "SIRS" observations. *Mon. Wea. Rev.*, **98**, 582-603.
- Twomey, S., 1963: On the numerical solution of Fredholm integral equations of the first kind by the inversion of the linear system produced by quadrature. *J. Assoc. Comp. Mach.*, **10**, 97-101.
- Wark, D. Q., 1970: SIRS, An experiment to measure the free air temperature from a satellite. *Appl. Opt.*, **9**, 1761-1766.
- , and D. T. Hilleary, 1969: Atmospheric temperature: Successful test of remote probing. *Science*, **165**, 1256-1258.